

Published in final edited form as:

Proc IEEE Conf Nanotechnol. 2008 August 18; 2008: 646–649. doi:10.1109/NANO.2008.196.

Magnetic Nanoparticles to Enhance Cell Seeding and Distribution in Tissue Engineering Scaffolds

Paul Thevenot¹, Syed Sohaebuddin¹, Narayan Poudyal², J. Ping Liu², and Liping Tang¹

Liping Tang: ltang@uta.edu

¹Department of Bioengineering, The University of Texas at Arlington, Arlington, TX

²Department of Physics, The University of Texas at Arlington, Arlington, TX

Abstract

The success of tissue engineering scaffolds is intimately linked with the ability of the seeded cells to adequately distribute and proliferate within the scaffold matrix. In tissue engineering scaffolds, it is difficult to achieve adequate distribution due to the hydrophobic nature of most scaffold materials and poor initial distribution following scaffold seeding. In this study, we investigated the distribution of cells in PLGA salt-leached scaffolds after seeding with magnetic nanoparticle loaded cells with a neodymium magnet placed below. The combined use of magnetic nanoparticle seeded cells and magnetic force was able to not only increase the total number of scaffold adherent cells, but also increase the infiltration and distribution compared with controls. This method to control the distribution of cells may provide a method to increase the functionality of tissue engineering scaffolds.

Keywords

magnetic nanoparticles; tissue engineering; seeding methods; cell distribution

I. Introduction

In recent years, much progress has been made in the field of regenerative medicine and tissue engineering. Efforts have focused on developing degradable tissue scaffolds to grow tissues *in vitro* with function and anatomical structure similar to native tissue. Investigators have attempted to engineer bone, cartilage, skin, and others for numerous clinical conditions. Unfortunately, most approaches have failed to produce solid tissue (>4 mm thickness) with limited cell distribution. Therefore, there is great interest in developing novel methods to facilitate cell migration and growth in thick scaffolds.

Several methods have been developed to enhance cell seeding in scaffolds. These include dynamic seeding methods and/or bioreactors to perfuse cell solutions through scaffold constructs, creating higher initial seeding densities while also increasing cell distribution [1]. However, these methods may either destroy the porous scaffold architecture or fail to produce tissue >2mm thickness.

Advances in nanotechnology have produced magnetic particles designed and tested for a variety of biological and medical applications as imaging contrast agents in cell sorting, bioseparation, drug targeting and the formation of cell sheets [2–5]. Recently, the use of magnetic nanoparticles to enhance cell seeding in tissue engineering scaffolds has been investigated [6]. It was demonstrated that cells could be loaded with magnetic nanoparticles and seeded onto porous scaffolds through the use of a magnetic field. Though magnetic nanoparticle seeding did increase the total scaffold-associated cells, the location and

distribution of the cells remains uninvestigated. If magnetic nanoparticle seeding is able to increase the ability of cells to enter the center portions of the scaffold and proliferate, the potential for complete 3D seeding of scaffolds may be realized. Therefore in this study, we sought to investigate the ability of magnetic nanoparticle loaded cells and magnetic force to cell penetration, distribution, and growth into tissue scaffold.

II. Materials and Methods

A. Synthesis of Magnetic FePt Nanoparticles

Magnetic L1₀ FePt nanoparticles of diameter 8 nm used in this investigation were prepared by two steps. First, disordered face-centered cubic (fcc) FePt nanoparticles of 8 nm diameter were prepared via chemical reduction of Pt(acac)₂ and thermal decomposition of Fe(CO)₅ by standard airless technique [7]. The as-synthesized fcc FePt nanoparticles with low magnetocrystalline anisotropy were then transformed to ordered L1₀ FePt nanoparticles with high magnetocrystalline anisotropy by a novel heat treatment technique. Details of preparation of L1₀ FePt nanoparticles by salt matrix annealing technique and their magnetic properties were reported previously [8, 9].

B. Cell Line and FePt Cellular Uptake and Toxicity

3T3 fibroblasts cells (ATCC) were expanded to the fourth passage and exposed to magnetic nanoparticles by direct addition of FePt magnetic nanoparticles suspended in serum free media. Before use particles were suspended in serum free DMEM and sonicated briefly to distribute. Based on published protocols, magnetic nanoparticles were added at a concentration of 100pg/cell, shown to be a non-toxic and efficient concentration for magnetic nanoparticle delivery with Fe₂O₃, followed by 4 hours of incubation [3,5]. Cell uptake was verified by Prussian blue staining of exposed cells adhered to coverslips.

To verify the effects of FePt on cell viability, 3T3 cells were exposed to 100pg/cell of FePt for 4 hours followed by removal of the nanoparticle containing media. Fresh media was replaced and viability analyzed by live/dead cytotoxicity/viability staining (Molecular Probes-Invitrogen, Carlsbad, CA). Live and dead total cell numbers were determined using Image J [10] and expressed as percent live cells relative to total cells.

C. PLGA Salt-Leached Scaffolds

Scaffolds were fabricated from PLGA (75:25, MW-135kDa). Scaffolds were prepared following established protocols. NaCl was used as the porogen and was sieved to a diameter of 250µm. Following fabrication, the salt was leached in distilled water and leaching verified by the absence of precipitate after addition of 0.1M silver nitrate. Scaffolds were viewed using SEM to verify porosity.

D. Scaffold Seeding and Magnet Application

FePt nanoparticle exposed 3T3 cells were thoroughly rinsed in PBS, trypsinized, and seeded at a density of 1×10^5 cells per scaffold. Scaffolds were sterilized in 70% EtOH, exchanged in PBS, and pre-wet with DMEM prior to seeding. Scaffolds were surface seeded by even distribution of 20µL of cell solution along one side (facing upward) of the scaffold. Immediately following seeding, a cylindrical neodymium magnet (diameter, 30mm; height, 15mm; magnetic induction, 4000G) was placed underneath the well plate (Fig. 1). The scaffolds were incubated for 3 hours to allow cell attachment, then submersed in DMEM with 10% FBS.

E. Analysis of Cell Infiltration and Distribution

Scaffolds were allowed to incubate for 3 days then processed as previously described [11]. Briefly, the cells adhered to the scaffolds were labeled with the cell tracer dye CFDA-SE (Invitrogen), fixed in cold methanol, embedded in OCT, and cryosectioned at 20 μ m. Sections were then organized, imaged, and compiled to a 3D image as previously described [11]. Additionally the cell distribution within each section was determined using a method established in our previous investigations [11]. Image J [10] was used along with the particle counter functionality, tuned to detect fluorescent cells in the images, to determine the number of cells per section. To determine cell density in the center of the scaffold sections, the sampling area was adjusted to a circle 10% of the total section area with origin at the center of the section. Additionally, Prussian blue staining was used to determine whether infiltrated cells contained FePt.

III. Results

A. FePt Cellular Uptake

Viability staining of exposed 3T3 cells at various time points revealed virtually no toxicity in comparison to control unexposed cells (Fig. 2). 3T3 cells seeded on coverslips and exposed to FePt nanoparticles for 4 hours were fixed and stained for Fe with Prussian blue with Nuclear Fast Red used as counterstain. Visualization and imaging using a Leica DMLB with 100X objective revealed areas staining positive with Prussian blue (blue particles) indicating that particles were either taken up by cells or adsorbed onto the surface of the cell (Fig. 3A–3B).

B. Cell Distribution and Infiltration Following Magnetic Force Seeding

Sections of both control scaffolds (FePt exposure without magnet application), and magnet exposed scaffolds (n=2 for both) were stained with fluorescent tracer dye, sectioned, imaged, and analyzed for total cells per section (Fig. 4A). Total cells were expressed as percentage of the total and compared for both methods (Fig. 4B). There appears to a slight increase in percentage total cells in the center and bottom of the magnet exposed scaffolds in comparison to control seeding. As expected, the majority of cells in control seeding are present at the location of seeding on the upper surface of the scaffold. Total cell values were then recorded based on scaffold section surface area (mm²) and compared among both methods through the depth of the scaffold (Fig. 4C). From this plot we can clearly visualize the differences in cell distribution as a result of magnet in conjunction with the FePt nanoparticles. The cell density along the seeded surface of the scaffold begins nearly equivalent for both methods. However, as we descend through the scaffold, the cell density is greatly enhanced in relation to control seeding, most importantly in the center portion of the scaffold.

We next analyzed images from the center of the scaffold to determine the cell distribution within these sections. The central section of the control scaffold without magnet application shows a high cell density at the top of the section corresponding to the seeded side of the scaffold (Fig. 5A). In contrast, the magnet seeded scaffold section (Fig. 5B) shows an even distribution of cells on the section and a high density of cells in the center of the section, representing the exact middle of the scaffold.

To distinguish if this increase in cell density was due to cells infiltrated into the center of the scaffold or along the outer edges, we specified a restricted counting area. An area focused in the center of the scaffold sections representing a 10% circular area of the total section area with origin at the center was counted to represent central density. From this plot, we are able to clearly see a drastic increase in central cell density in comparison to control seeding (Fig.

5C). For control seeding, almost no cells are present in the middle of the central sections, with cell densities less than 10 cells/mm². For magnet seeding, central values range from 100–200 cells/mm², representing more than a 10-fold increase in density in the center of the scaffold.

To determine if these infiltrated cells were due to FePt uptake and magnetic force, center sections were stained with Prussian blue and counterstained in Nuclear Fast Red to visualize FePt particles (Fig. 6). The images show scaffold associated cells staining positive for FePt as labeled in the image (Fig. 6A) with an inverse image indicating the scaffold and cell (Fig. 6B). The positively stained particles can also be seen in a cluster of cells adhered to the scaffold (Fig. 6C), with the scaffold and cells indicated specifically in the accompanying inverse image (Fig. 6D).

IV. Discussion

Many tissue engineering products have achieved measurable levels of success in regenerating damaged or diseased tissues. However, most successes have been with thin tissues or are not to clinical scale. One reason for this limited process is the ability to adequately construct 3D tissue matrices that resemble physiological tissues. A contribution to this is the difficulty in establishing homogeneously seeded tissues in vitro. The goal of this study was to expand upon previous works by other groups which has shown that magnetic nanoparticle loaded cells, coupled with the application of magnetic force, can lead to more scaffold associated cells. In this study, we have attempted to characterize whether this process is able to infuse cells throughout the matrix, especially into the central regions of the scaffold, and whether these cells will survive at that location and potentially proliferate.

Using FePt nanoparticles, which have shown some superior properties compared to Fe₂O₃, we have shown that these particles are able to associate with cells, though it is unclear whether they are taken up and temporarily stored by the cells or adsorbed to the cell membrane. Through this association, we are able to draw cells to the scaffold in a more efficient manner than can be achieved through static seeding, as previously established with Fe₂O₃. Through careful observation of the scaffold architecture and the adherent cells, it can also be seen that these cells were not only kept on the scaffold, but were also able to infiltrate through the matrix and deposit/adhere throughout the matrix in manner that may not be possible through traditionally static seeding. It was also seen that the cells located within the central portions of the matrix were indeed FePt associated cells. Thus there appears potential that this method may provide a useful method to homogeneously seed tissue engineering scaffolds without effecting the viability and functionality of the cells. Though parameters of magnetic force would need adjusting, it may be possible to adequately seed clinically sized constructs and possibly enhance their functionality by both distributing and constituting cells similar to physiological tissues and also controlling their location and organization in relation to other cells.

V. Conclusion

Seeding tissue engineering scaffolds through the use of cell associated magnetic nanoparticles and magnetic force appears to be a successful method to increase the number of scaffold associated cells. In addition, this method also can increase the infiltration and distribution of cells within the matrix and has potential to assist the development of more physiological tissues in vitro. Additionally, this method may be useful in controlling the distribution of multiple cell types within constructs and have applications in cell alignment and matrix deposition necessary for the physiological function of many tissues such as muscles and ligaments.

Acknowledgments

Research is funded by a grant from NIH, GM074021

References

1. Zhao F, Ma T. Perfusion bioreactor system for human mesenchymal stem cell tissue engineering: dynamic seeding and construct development. *Biotechnol Bioeng.* 2005; 91(4):482–493. [PubMed: 15895382]
2. Ito A, Hibino E, Shimizu K, Kobayashi T, Yamada Y, Hibi H, Ueda M, Honda H. Magnetic force-based mesenchymal stem cell expansion using antibody-conjugated magnetoliposomes. *J Biomed Mater Res B Appl Biomater.* 2005; 75(2):320–327. [PubMed: 16025453]
3. Ito A, Kuga Y, Honda H, Kikkawa H, Horiuchi A, Wantanabe Y, Kobayashi T. Magnetic nanoparticle-loaded anti-HER2 immunoliposomes for combination of antibody therapy with hyperthermia. *Cancer Lett.* 2004; 212(2):167–175. [PubMed: 15279897]
4. Campbell RB. Battling tumors with magnetic nanotherapeutics and hyperthermia: turning up the heat. *Nanomed.* 2007; 2(5):649–652.
5. Shimizu K, Ito A, Yoshida T, Yamada Y, Ueda M, Honda H. Bone tissue engineering with human mesenchymal stem cell sheets constructed using magnetite nanoparticles and magnetic force. *J Biomed Mater Res B Appl Biomater.* 2007; 82(2):471–480. [PubMed: 17279563]
6. Shimizu K, Ito A, Lee JK, Yoshida T, Miwa K, Ishiguro H, Numaguchi Y, Murohara T, Kodama I, Honda H. Construction of multi-layered cardiomyocyte sheets using magnetite nanoparticles and magnetic force. *Biotechnol Bioeng.* 2006; 96(4):803–809. [PubMed: 16865728]
7. Nandwana V, Elkins KE, Poudyal N, Chaubey GS, Yano K, Liu JP. Size and shape control of monodisperse FePt nanoparticles with giant coercivity. *J Phys Chem C.* 2007; 111:4185–4189.
8. Elkins K, Li D, Poudyal N, Nandwana V, Jin Z, Chen K, Liu JP. Monodisperse face-centred tetragonal FePt nanoparticles with giant coercivity. *J Phys D: Appl Phys.* 2005; 38:2306–2309.
9. Rong C, Li D, Nandwana V, Poudyal N, Ding Y, Wang Z, Zeng H, Liu JP. Size-dependent chemical and magnetic ordering in L1₀ FePt nanoparticles. *Adv Mater.* 2006; 18:2984–2988.
10. Abramoff MD, Magelhaes PJ, Ram SJ. Image processing with ImageJ. *Biophotonics Int.* 2004; 11(7):36–42.
11. Thevenot, P.; Tang, T. Novel method to monitor cell survival and distribution in PLGA degradable scaffolds. *IEEE Dallas Engineering in Medicine and Biology Workshop*; November 2007; Dallas, TX.

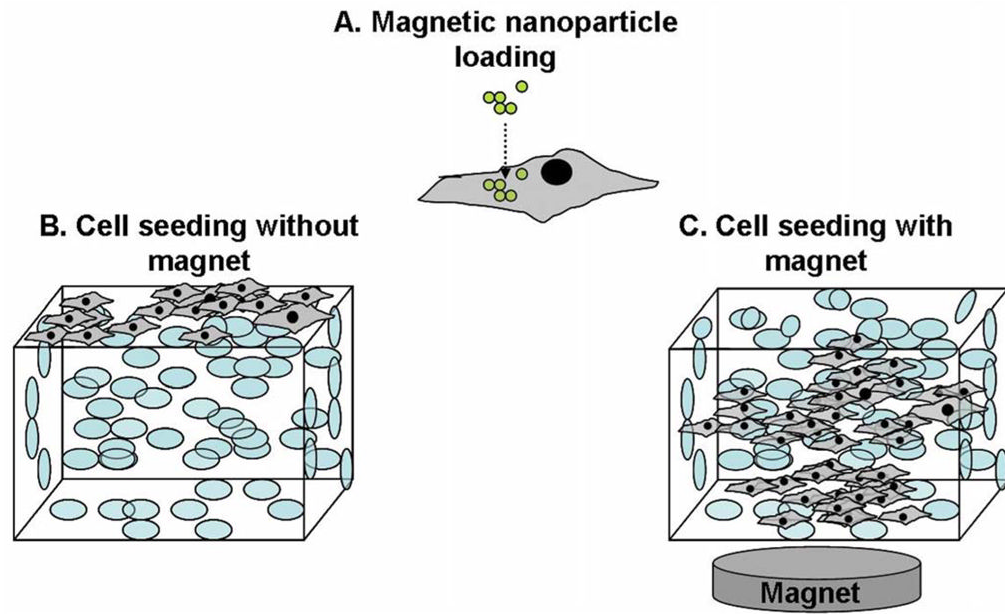


Figure 1. Scaffold seeding diagram. (A) 3T3 cells loaded with magnetic nanoparticles. (B) Control scaffolds surface seeded without the magnet. (C) Scaffolds seeded with immediate application of a magnet below to draw the cells into the scaffold.

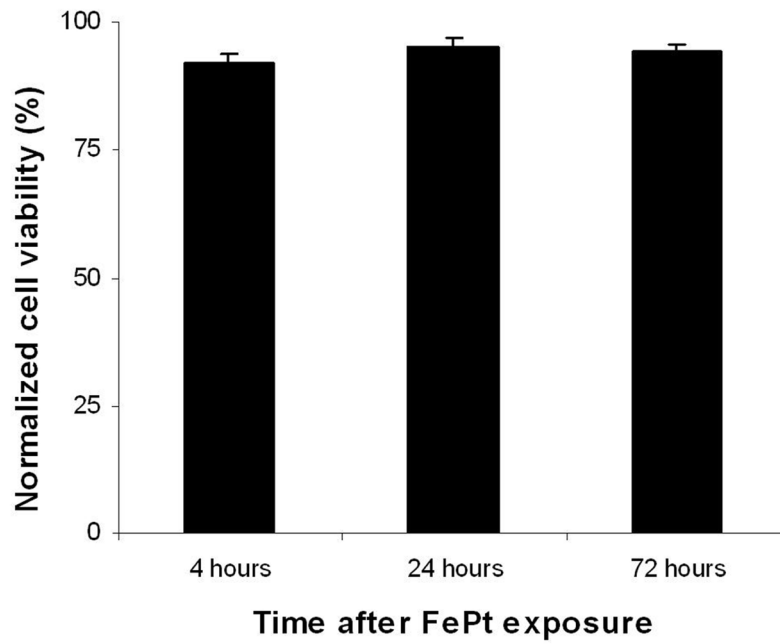


Figure 2. Effect of FePt nanoparticle uptake on 3T3 viability. Cells were exposed to 100pg/cell for 4 hours after which the media containing the particles was removed. Cells were viability stained at 4, 24, and 72 hours after particle exposure.

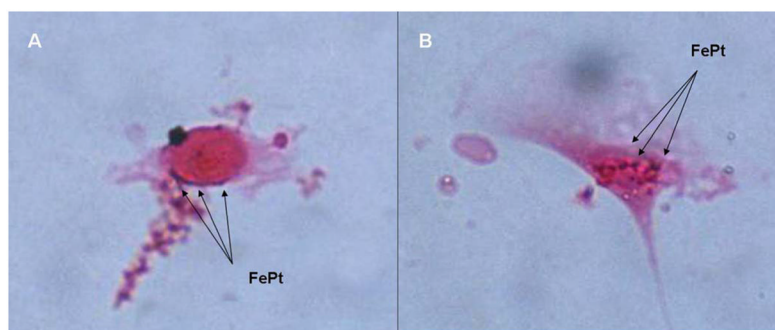


Figure 3. FePt particle uptake by 3T3 cells after 4 hours of exposure in serum free media with Prussian blue staining of iron and counterstain with Nuclear Fast Red. (A) FePt (blue) can be observed along the edges of the cell membrane and in some cases (B) on top of the cell.

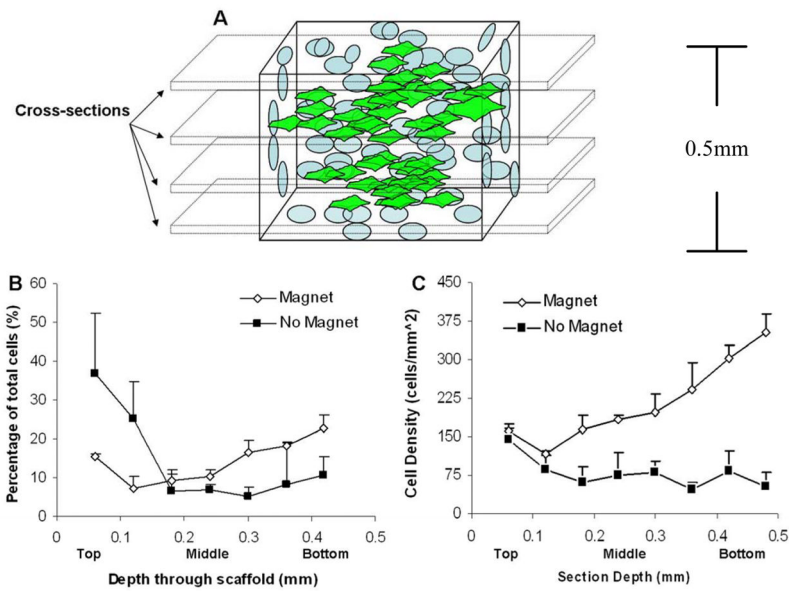


Figure 4.

Live cell distribution vertically through the scaffold. Scaffolds were stained for live cells, cross-sectioned, and imaged for live cell fluorescence. (A) Schematic of sectioning procedure. (B) Cell distribution through the scaffold expressed as a percentage of total cells in the scaffold. (C) Cell distribution through the scaffold expressed as a cell density relative to the scaffold section area.

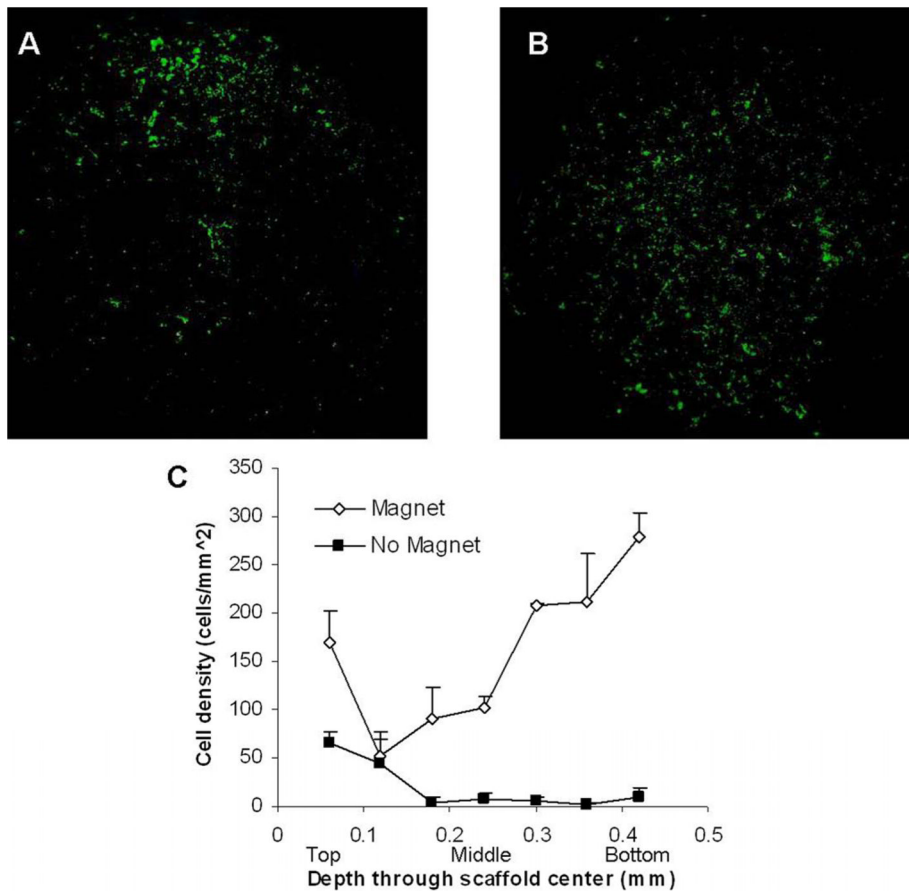


Figure 5.

Cell infiltration into the scaffold. (A) Cross-section image of the center of the scaffold seeded without application of the magnetic, showing cell concentrated on the seeded surface of the scaffold with little penetration. (B) Cross-section of the seeded scaffold with magnet application showing and even cell distribution throughout the center section of the scaffold. (C) Plot of cell density in 10% circle area with origin at the center of the scaffold sections vertically through the scaffold depicting enhanced cell distribution in the center of the scaffold after magnet application.

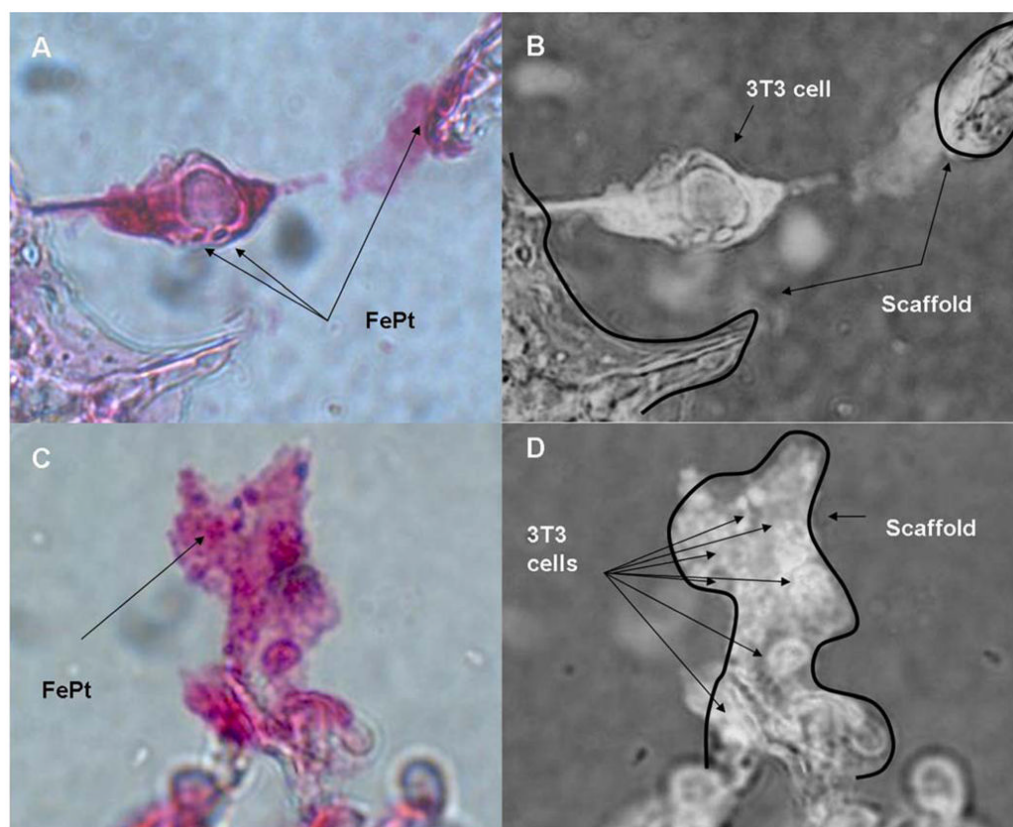


Figure 6.

Presence of FePt particles with cells in the center section magnet applied scaffolds. (A) Prussian blue stain with counterstain of Nuclear Fast Red with positive stained FePt particles indicated as blue. (B) Inverse of (A) indicating the 3T3 cell spanning between two portions of the scaffold indicated by arrows. (C) Group of cells adhered along the scaffold with Prussian Blue stained FePt visible on the cluster of cells. (D) Inverse of image (C) showing the structure of the scaffold with arrows pointing toward the individual cells in the cluster.